Performance Comparison of Device-to-Device Mode Selection Schemes

Daniel Marshall, Salman Durrani, Jing Guo and Nan Yang
Research School of Engineering, The Australian National University, Canberra, ACT 2601, Australia.
Corresponding author email: salman.durrani@anu.edu.au.

***Abstract*—In this paper, we build a unified analytical framework that allows for analysis and comparison of three device-to-device (D2D) mode selection schemes proposed in the literature to date, namely the distance cut-off scheme, the link gain scheme and the guard zone scheme. In the framework we adopt Poisson point process (PPP) assumptions to model the cellular and D2D interference, respectively. Using stochastic geometry, we derive easy to implement expressions for the success probability at a typical base station (BS) and a typical D2D receiver (RX) in an underlay in-band D2D-enabled single tier cellular network. Comparing the derived analytical results with simulations, we show that the PPP assumptions are accurate for the success probability at the BS. Moreover, they provide a good approximation for the success probability at the D2D RX when the D2D RX is located close to the cell edge. Furthermore, the distance cut-off scheme generally outperforms other mode selection schemes.**

I. Introduction

Device-to-device (D2D) communication is envisaged to play a key role in enabling 5G wireless systems [1], [2]. By allowing two or more user equipments (UEs) to bypass the base station (BS) and communicate directly with each other, D2D communication improves the spectrum utilization and overall throughput [3], [4]. In this paper, we consider underlay in-band D2D communications, where the D2D transmitters are allowed to share the same spectrum resources with cellular users. A key research challenge in underlay in-band D2D networks is interference management. Due to the concurrent transmission on the same spectrum, D2D users cause both inter-cell and intra-cell interference to the cellular users, which can adversely affect cellular network performance. In this regard, advanced, sophisticated solutions for interference management have been proposed, which involve adaptively limiting D2D transmit power based on local cellular transmitters [5], a centralized opportunistic access control scheme [6], or a centralized and distributed power control algorithm [7].

A simple yet effective solution to interference management in underlay in-band D2D networks is through mode selection schemes, which govern whether the D2D UEs choose D2D mode or operate in an alternative transmission mode. Some research papers have proposed mode selection schemes (e.g., [8]–[11]), assuming that the location of users is fixed. However, in practice the location of users is random, which impacts both the mode selection scheme and the network performance. Stochastic geometry provides a powerful mathematical tool to capture and study the randomness of UEs. Recently, some papers have proposed mode selection schemes taking the random user locations into account and analyzed the resulting network performance using stochastic geometry. A distance based scheme was proposed in [12]. An instantaneous link gain based scheme was proposed in [13], while a guard zone based scheme was proposed in [14]. However, [12]–[14] used different system model assumptions and approximations. Hence, it is important to develop an analytical framework to allow for a fair comparison of these mode selection schemes.

In this paper, we use stochastic geometry and present a unified analytical framework for comparison of D2D mode selection schemes in an underlay in-band D2D-enabled single tier cellular network. The novel contributions are:

- We use Poisson point process (PPP) assumptions to model the cellular and D2D interference, respectively, and derive the success probability at a typical BS and a typical D2D receiver (RX) for the distance cut-off scheme, the link gain scheme and the guard zone scheme.
- We use system level simulations to critically assess the accuracy of the derived analytical results. Our results show that the PPP assumptions are accurate for the success probability at the BS. However, for the D2D RX the PPP assumptions only provide a good approximation when the D2D RX is located near the cell edge. To the best of our knowledge, such an analysis on the accuracy of the stochastic geometry results for D2D networks has not been reported in the literature to date.
- We compare the performance of the three mode selection schemes. The results show that the distance cut-off scheme generally achieves the highest D2D RX success probability, while maintaining the intensity of D2D UEs in D2D mode as large as possible, for a given success probability at the BS.

II. System model

We consider a D2D-enabled single (macro) tier cellular network, where the BSs are regularly placed on a hexagonal grid. The use of hexagons to model cells in cellular networks is well established in the literature [12], [14], [15]. The lattice has intensity λ_b, i.e., the area of each hexagonal cell is $\frac{1}{\lambda_b}$. The cellular UEs are modelled in $\mathbb{R}^2$ by a homogeneous PPP with intensity λ_u, where $\lambda_u >> \lambda_b$. There are also some potential D2D transmitters, which are modelled by an independent PPP with intensity λ_d. Note that the word 'potential' indicates that these D2D transmitters have the option of bypassing the BS and communicating directly with their intended receivers (known as the D2D mode) or the using other transmission mode, according to the mode selection scheme. The other transmission mode can be the cellular mode or it can also be the out-band mode, i.e., D2D operating in the unlicensed spectrum band. However, the main focus of this paper are

978-1-4673-6782-0/15/$31.00 ©2015 IEEE

the D2D transmitters in the D2D mode. Hence, in this paper, we assume that the D2D transmitters only in D2D mode can transmit. In the following, we refer to the D2D transmitters in D2D mode as D2D UEs.

We assume that individual and orthogonal channels are assigned to each cellular UE in a macrocell. Thus, there is no intra-cell interference from cellular UEs within the same cell. However, there is universal frequency re-use across the cellular network leading to inter-cell interference. The D2D UEs coexist in an uplink channel with the cellular UEs. Hence, they cause both intra-cell and inter-cell interference at the BSs and other D2D UEs. Therefore, we focus on one uplink channel experiencing inter-cell interference from cellular UEs and inter-cell and intra-cell interference from D2D UEs. Additionally, the density of cellular UEs is far greater than the density of BSs such that there is at least one cellular UE occupying the considered uplink channel. For analytical tractability, we model the location of cellular UEs using the considered uplink channel in different cells as a PPP with density λ_b [12], [14], denoted as Φ_c.

Channel and Link Distance Models: We assume all links experience path-loss plus Rayleigh fading. In this way, the received power at a typical RX can be expressed as $\rho = Pr^{-\alpha}G$, where P is the transmit power from a transmitter, r denotes the link distance and $\alpha > 2$ is the path-loss exponent [15]. Let α_c and α_d denote the path-loss exponent on the cellular link and D2D link, respectively. G represents the independently and identically distributed (i.i.d.) Rayleigh fading power gain, which follows exponential distribution with unit mean. All links also experience AWGN noise with variance σ^2.

The cellular UEs and D2D UEs are equipped with a single antenna each and transmit with power P_c and P_d, respectively. All UEs use truncated channel inversion power control [12] to maintain an average signal power equal to ρ at the intended RX. The D2D UEs have a maximum transmit power P_u. For analytical convenience, we approximate the macrocells by disks of radius R, where R is related to area by $\frac{1}{\lambda_b} = \pi R^2$ [12]. Due to the PPP assumption, both the cellular UEs and potential D2D transmitters can be regarded as uniformly distributed in the cell. Hence, the probability distribution function (pdf) of its distance to the BS r_c is given by

$$f_{r_c}(r_c) = \frac{2r_c}{R^2}, \quad 0 \le r_c \le R. \tag{1}$$

For each potential D2D transmitter, we further assume there is an intended D2D RX surrounding it. In terms of the D2D link distance r_d, it is modelled by a Rayleigh distribution with pdf $f'_{r_d}(r_d) = 2\pi\lambda_d r_d \exp\left(-\pi\lambda_d r_d^2\right)$. Note that this distribution generally describes the distance between a point and its nearest neighbour in a Poisson distribution [16]. Due to the maximum power constraint and power control, the maximum distance at which D2D UEs can communicate is given by $R_{\max} = (\frac{P_u}{\rho})^{\frac{1}{\alpha_d}}$. It is further assumed that the intended D2D UE RX is located within this range. Therefore, the exact pdf is normalised by $R_{\max}$ as

$$\begin{aligned} f_{r_d}(r_d) &= \frac{f'_{r_d}(r_d)}{\mathbb{P}(r_c < R_{\max})} \\ &= \frac{2\pi\lambda_d r_d \exp\left(-\pi\lambda_d r_d^2\right)}{1 - \exp\left(-\pi\lambda_d R_{\max}^2\right)}, \quad 0 \le r_d \le R_{\max}. \end{aligned} \tag{2}$$

We assume that the D2D UEs have the location information of the BS and the intended D2D RX. Also, the BS and UEs have access to perfect channel state information (CSI). This assumption allows benchmark performance to be determined.

Mode Selection: In this work we consider and compare three mode selection schemes from the literature. We use $\mathcal{M} = 1, 2, 3$ to denote the three schemes.

- The first scheme ($\mathcal{M} = 1$) is a *distance cut-off* scheme [12]. A potential D2D transmitter chooses the D2D mode if $r_d < \gamma$, where γ is a threshold distance;
- The second scheme ($\mathcal{M} = 2$) is a *link gain* scheme [13]. A potential D2D transmitter chooses the D2D mode if the biased D2D link quality is at least as good as the cellular uplink link quality, i.e., if $r_c^{-\alpha_c} < T_d r_d^{-\alpha_d}$ where T_d is a bias factor and r_c and r_d are defined before (1) and (2);
- The third scheme ($\mathcal{M} = 3$) is a *guard zone* scheme [14]. A potential D2D transmitter chooses the D2D mode if cellular link distance is greater than the guard distance, i.e. $r_c > R_g$, where R_g is the guard zone radius.

III. Unified Analytical Framework

We consider a typical RX (BS or D2D RX), which is assumed to be located at the origin[1]. For a certain mode selection scheme, the SINR experienced at a typical RX κ (BS or D2D RX) is given by

$$SINR^{\kappa} = \frac{\rho G_0}{I_c^{\kappa} + I_d^{\kappa} + \sigma^2}, \tag{3}$$

where I_c^{κ} represents the aggregate interference experienced at RX κ from cellular UEs using the same uplink channel in different macrocells, I_d^{κ} is the aggregate interference experienced at RX κ from D2D UEs located anywhere, including both inter-cell and intra-cell, and σ^2 is the power of the AWGN noise. Note that the average received signal power from the intended transmitter is always the same due to channel inversion, and only varies due to the effect of Rayleigh fading power gain G_0. Here G_0 is also exponentially distributed and the subscript 0 is used to distinguish it from the fading power gain on the interference link.

In this paper, we examine the network performance using the success probability, which is defined as the average probability that the SINR at the typical RX κ is greater than a

[1]Since the location of interfering cellular UEs is approximated by PPP, by Slivnyak's theorem, the performance at this typical BS reflects the performance at other BSs. However, in reality the location of interfering D2D UEs does not strictly follow the PPP and the success probability at the D2D RX is location-dependent, especially for the *guard zone* scheme. For analytical convenience, we still assume the location of interfering D2D UEs follows a PPP and we will see the effect of this approximation in Section IV.

certain SINR threshold θ. It is mathematically written as

$$\begin{aligned}\mathbb{P}^{\kappa}_{suc} &= \mathbb{P}(SINR^{\kappa} \geq \theta) = \mathbb{P}\left(\frac{\rho G_0}{I^{\kappa}_c + I^{\kappa}_d + \sigma^2} \geq \theta\right) \\ &= \mathbb{E}_{I^{\kappa}_c, I^{\kappa}_d}\left[1 - F_{G_0}\left(\frac{\theta}{\rho}\left(I^{\kappa}_c + I^{\kappa}_d + \sigma^2\right)\right)\right] \\ &= \exp\left(-\frac{\theta}{\rho}\sigma^2\right)\mathcal{L}_{I^{\kappa}_c}\left(\frac{\theta}{\rho}\right)\mathcal{L}_{I^{\kappa}_d}\left(\frac{\theta}{\rho}\right), \end{aligned} \quad (4)$$

where $\mathbb{E}_{I^{\kappa}_c, I^{\kappa}_d}[\cdot]$ denotes the expectation operator with respect to the aggregate interference from cellular UEs and D2D UEs, $\mathcal{L}_{I^{\kappa}_c}(\cdot)$ and $\mathcal{L}_{I^{\kappa}_d}(\cdot)$ are the Laplace transform of the pdf of I^{κ}_c and I^{κ}_d, respectively. Note that the last step in (4) comes from using the exponential distribution of G_0 and the definition of the Laplace transform of a random variable's distribution. It can be seen that the success probability is broken down into three multiplicative components, which can be calculated separately. Before presenting these success probability results, we summarize three important lemmas which help to determine the Laplace transform of the pdf of I^{κ}_c and I^{κ}_d.

A. Probability of being in D2D mode

Lemma 1: The probability of a potential D2D UE choosing D2D mode under mode selection scheme $\mathcal{M}$, with D2D link distance $f_{r_d}(r_d)$ in (2) and BS distance $f_{r_c}(r_c)$ in (1), is

$$\mathbb{P}_{D2D} = \begin{cases} \frac{1-\exp\left(-\pi\lambda_d\gamma^2\right)}{1-\exp\left(-\pi\lambda_d R^2_{max}\right)}, & \mathcal{M}=1; \\ \frac{1-\exp\left(-\pi\lambda_d \min\left(R^{\frac{2\alpha_c}{\alpha_d}} T_d^{\frac{2}{\alpha_d}}, R^2_{max}\right)\right)}{1-\exp\left(-\pi\lambda_d R^2_{max}\right)} \\ \quad - \frac{\gamma\left(\frac{\alpha_d}{\alpha_c}+1, \pi\lambda_d \min\left(R^{\frac{2\alpha_c}{\alpha_d}} T_d^{\frac{2}{\alpha_d}}, R^2_{max}\right)\right)}{(\pi\lambda_d)^{\frac{\alpha_d}{\alpha_c}} R^2 T_d^{\frac{2}{\alpha_c}} \left(1-\exp\left(-\pi\lambda_d R^2_{max}\right)\right)}, & \mathcal{M}=2; \\ 1 - R_g^2/R^2, & \mathcal{M}=3; \end{cases} \quad (5)$$

where $\gamma(s,x) = \int_0^x t^{s-1}e^{-t}\mathrm{d}t$ is the lower incomplete gamma function and $\min(\cdot,\cdot)$ denotes the minimum value.

Proof: The probability is determined by finding the expected value of $\mathbb{P}$(D2D mode condition), where the condition is provided in the mode selection in Section II. This can be evaluated by integrating the probability distribution across the range of r_c and r_d. For example, for $\mathcal{M} = 2$, the D2D mode condition is $r_c^{-\alpha_c} < T_d r_d^{-\alpha_d}$. Then $\mathbb{P}_{D2D} = \mathbb{E}_{r_d, r_c}\left[\mathbb{P}\left(r_c^{-\alpha_c} < T_d r_d^{-\alpha_d}\right)\right]$. Substituting the distribution of r_d and r_c, we can obtain the result shown in (5). ∎

B. Transmit Power of UEs

By employing channel inversion power control, the power of a transmitting UE is always modified such that $Pr^{-\alpha} = \rho$, or equivalently, $P = \rho r^{\alpha}$. As the distance distributions for r (i.e., r_d and r_c) are known, the average transmit power can be found. Here, the n^{th} moment of the transmit powers are characterized, as these form important components of later calculations.

Lemma 2: For any cellular UE, the n^{th} moment of the transmit power P_c is given by

$$\mathbb{E}[P_c^n] = \frac{2\rho^n R^{n\alpha_c}}{n\alpha_c + 2}. \quad (6)$$

Proof: This average transmit power is obtained by evaluating the integral $\mathbb{E}[P_c^n] = \mathbb{E}[\rho^n r^{n\alpha_c}] = \int_0^R \rho^n r^{n\alpha_c} f_{r_c}(r)\mathrm{d}r$ and simplifying. ∎

Lemma 3: For a potential D2D UE operating in D2D mode, the n^{th} moment of the transmit power P_d is given by

$$\mathbb{E}[P_d^n] = \frac{(\pi\lambda_d)^{-\frac{n\alpha_d}{2}}\rho^n}{1-\exp\left(-\pi\lambda_d R^2_{max}\right)}\gamma\left(\frac{n\alpha_d}{2}+1, \pi\lambda_d R^2_{max}\right) \quad (7)$$

Proof: The average transmit power for D2D UEs is obtained by evaluating the integral $\mathbb{E}[P_d^n] = \mathbb{E}[\rho^n r^{n\alpha_d}] = \int_0^{R_{\max}} \rho^n r^{n\alpha_d} f_{r_d}(r)\mathrm{d}r$ and simplifying. ∎

Remark 1: A special case exists for the *distance cut-off* scheme. In this scheme, the maximum link distance r_d (and thus the maximum power) is limited by the cut-off parameter γ. As such, the moments of the transmit power under this scheme are obtained by substituting $R_{\max} = \gamma$ in (7).

C. Success Probability

We now present the two main results in this paper.

Theorem 1: For a D2D-enabled single tier cellular network operating under any of the three mode selection schemes, the success probability experienced at a typical D2D RX is given by (8), which is shown at the top of next page, where the probability of being in D2D mode $\mathbb{P}_{D2D}$ and the n^{th} moment of transmission power are given in (5) and (6)-(7), respectively. Note that, for the *guard zone* scheme, we need to replace $\mathbb{P}_{D2D}\lambda_d$ by λ_d, since the intensity of interfering D2D UEs is assumed to be λ_d for this case.

Proof: See Appendix A. ∎

Theorem 2: For a D2D-enabled single tier cellular network operating under any of the three mode selection schemes, the success probability experienced at a typical BS for a generic cellular UE is given by (9) which is shown at the top of next page, where the value of $A_{\mathcal{M}}$ depends on $\mathcal{M}$ as shown in (10). The probability of being in D2D mode $\mathbb{P}_{D2D}$ and the n^{th} moment of transmission power are given in (5) and (6)-(7) respectively.

Proof: See Appendix B. ∎

Remark 2: The result for $\mathcal{M} = 3$ cannot be expressed in closed-form. However, the values can be easily evaluated numerically. Also, (8) and (9) are valid for any α_c, α_d values.

IV. Results and Discussions

In this section, we examine the accuracy of the analytical results derived in *Theorem 1* and *Theorem 2*. We also compare the performance of the three mode selection schemes. Unless otherwise stated, the following parameters are used [12], [13]: $\lambda_b = 1.5$ BSs/km^2, $\lambda_d = 25$ UEs/km^2, $P_u = 200$ mW, $\rho = -70$ dBm, $\alpha_c = 4$, $\alpha_d = 4.5$, $\theta = 0$ dB and $\sigma^2 = -130$ dBm.

Accuracy of the analytical results: Fig. 1 plots the success probability versus the SINR threshold θ for different mode selection schemes with $\gamma = R_{\max}/2$, $T_d = 2$ and $R_g = 200$.

$$\mathbb{P}_{suc}^{\text{D2D}} = \exp\left(-\frac{\theta}{\rho}\sigma^2 - \pi\left(\frac{\theta}{\rho}\right)^{\frac{2}{\alpha_d}}\Gamma\left(1+\frac{2}{\alpha_d}\right)\Gamma\left(1-\frac{2}{\alpha_d}\right)\left(\lambda_b\mathbb{E}\left[P_c^{\frac{2}{\alpha_d}}\right]+\mathbb{P}_{D2D}\lambda_d\mathbb{E}\left[P_d^{\frac{2}{\alpha_d}}\right]\right)\right), \tag{8}$$

$$\mathbb{P}_{suc}^{\text{BS}} = \exp\left(-\frac{\theta}{\rho}\sigma^2 + \frac{\pi\lambda_b R^2\theta}{(2-\alpha_c)(2+\alpha_c)}\left((2+\alpha_c){}_2F_1\left(1,1-\frac{2}{\alpha_c};2-\frac{2}{\alpha_c};-\theta\right)+(2-\alpha_c){}_2F_1\left(1,1+\frac{2}{\alpha_c};2+\frac{2}{\alpha_c};-\theta\right)\right)+A_{\mathcal{M}}\right), \tag{9}$$

$$A_{\mathcal{M}} = \begin{cases} -\pi\mathbb{P}_{D2D}\lambda_d\mathbb{E}\left[P_d^{\frac{2}{\alpha_c}}\right]\left(\frac{\theta}{\rho}\right)^{\frac{2}{\alpha_c}}\Gamma\left(1+\frac{2}{\alpha_c}\right)\Gamma\left(1-\frac{2}{\alpha_c}\right), & \mathcal{M}=1; \\ -\frac{2\pi\mathbb{P}_{D2D}\lambda_d\mathbb{E}\left[P_d^{\frac{2}{\alpha_c}}\right]\theta T_d^{1-\frac{2}{\alpha_c}}\rho^{-\frac{2}{\alpha_c}}}{\alpha_c-2}{}_2F_1\left(1,1-\frac{2}{\alpha_c};2-\frac{2}{\alpha_c};-\theta T_d\right), & \mathcal{M}=2; \\ -\frac{4\pi^2\lambda_d^2\theta}{(\alpha_c-2)\left(1-\exp\left(-\pi\lambda_d R_{max}^2\right)\right)}\int_0^{R_{\max}}\Big(r^{\alpha_d+1}\exp\left(-\pi\lambda_d r^2\right)R_g^{2-\alpha_c}{}_2F_1\left(1,1-\frac{2}{\alpha_c};2-\frac{2}{\alpha_c};-\theta r^{\alpha_d}R_g^{-\alpha_c}\right) & \\ \quad -(1-\mathbb{P}_{D2D})\,r^{\alpha_d+1}\exp\left(-\pi\lambda_d r^2\right)(2R-R_g)^{2-\alpha_c}{}_2F_1\left(1,1-\frac{2}{\alpha_c};2-\frac{2}{\alpha_c};-\theta r^{\alpha_d}(2R-R_g)^{-\alpha_c}\right)\Big)\,\mathrm{d}r, & \mathcal{M}=3; \end{cases} \tag{10}$$

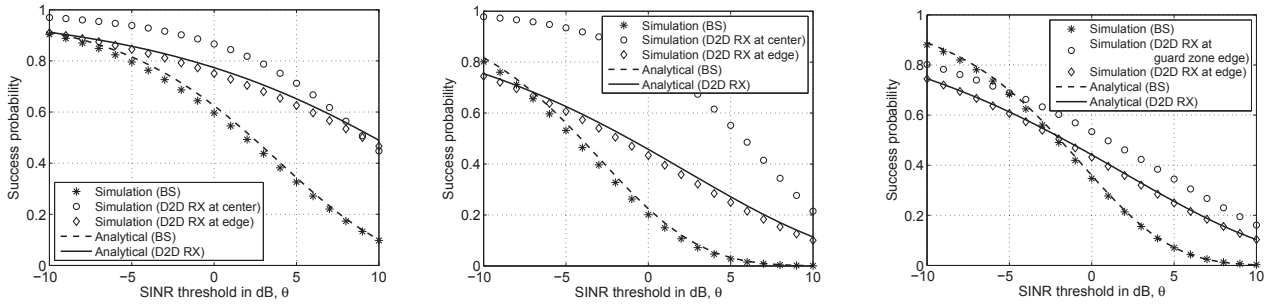

(a) *Distance cut-off* scheme ($\mathcal{M}=1$). (b) *Link gain* scheme ($\mathcal{M}=2$). (c) *Guard zone* scheme ($\mathcal{M}=3$).

Fig. 1. The success probability versus the SINR threshold θ for different mode selection scheme.

The analytical curves are plotted using *Theorem 1* and *Theorem 2*. We also generate the simulation results to examine the accuracy of the PPP assumptions for interfering cellular UEs and D2D UEs. For the D2D RX, the simulation results are generated for two cases (for a typical D2D RX close to the BS/guard zone edge and a typical D2D RX is close to the cell edge). As illustrated in Fig. 1, for the success probability at the BS, the derived analytical results match closely with the simulations, which demonstrates the accuracy of the adopted approximations.

For the success probability at the D2D RX, the analytical results are close to the simulation results when the D2D RX is at the cell edge, while they deviate from the simulation results when D2D RX is close to cell center/guard zone edge. For the *distance cut-off* scheme, this gap is mainly caused by the PPP assumption of interfering cellular UEs. Due to the orthogonal channel allocation, it is not possible to have more than one nearby interfering cellular UE for the cell-center-located D2D RX and the dominant interference is coming from the cellular UE residing in the same cell. However, the cell-edge-located D2D RX is likely to experience the dominant interference from at most three nearby cellular UEs. Since the PPP assumption allows more than one nearby interferer, it provides a good approximation for the case where the D2D RX is at the cell edge. For the *link gain* and *guard zone* schemes, the mismatch comes from both of the PPP assumptions for interfering cellular UEs (as explained previously) and interfering D2D UEs. The location of D2D UEs does not follow a PPP since the interfering D2D UEs are likely to be far away from the BSs. Hence, the cell-center-located (or guard-zone-edge-located) D2D RX experiences less interference from D2D UEs.

Comparison of mode selection schemes: We investigate and compare the mode selection schemes in terms of their effect on the BS (i.e., the success probability at BS) and the D2D UEs (i.e., the success probability at the cell-edge-located D2D RX, which is the worst case scenario). Fig. 2 plots the success probability at the D2D RX versus the success probability at the BS. The following approach is adopted to work out the curves [17]: for each $\mathbb{P}_{suc}^{\text{BS}}$ value, the values of γ, T and R_g can be found for different schemes using *Theorem 2*. By substituting these values into Theorem 1, $\mathbb{P}_{suc}^{\text{D2D}}$ is obtained. From the figure, we can see that under the same value of $\mathbb{P}_{suc}^{\text{BS}}$, the *distance cut-off* scheme has the highest $\mathbb{P}_{suc}^{\text{D2D}}$, followed by the *guard zone* scheme and *link gain* scheme. The main reason is that less 'potential' D2D UEs are in D2D mode, thereby reducing the interference at the D2D RX for *distance cut-off* scheme. We have also examined other system parameters (i.e., λ_b, λ_d, α_c, α_d and ρ) and found that in general this ordering stays the same, except for very high BS intensity. For very high λ_b, the *guard zone* scheme has slightly higher $\mathbb{P}_{suc}^{\text{D2D}}$ than

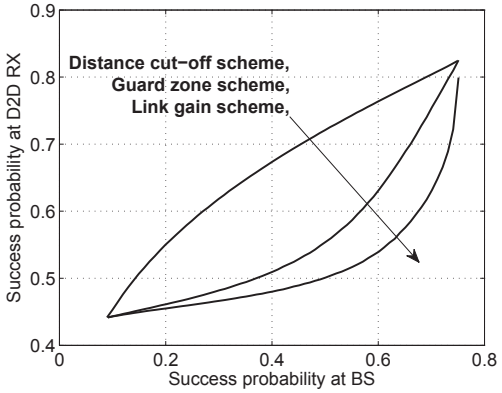

Fig. 2. The success probability at the D2D RX versus the success probability at the BS.

the *distance cut-off* scheme, then followed by the *link gain* scheme. These results are not included here for brevity.

V. Conclusions

We presented a unified analytical framework for comparison of D2D mode selection schemes using stochastic geometry. The results showed that the PPP assumptions for interfering cellular UEs and interfering D2D UEs are accurate for the success probability at the BS. However, the success probability at the D2D RX is accurate only when the D2D RX is located close to the cell edge. Additionally, the distance cut-off scheme generally outperforms other mode selection schemes.

Appendix A
Success Probability at a D2D Receiver

In this appendix, we show how (4) can be evaluated for a typical D2D RX. First, we consider the interference from cellular UEs. Using the Laplace transform definition, we have

$$\mathcal{L}_{I_c^{\mathrm{D2D}}}(s)=\mathbb{E}\left[\exp\left(-sI_c^{\mathrm{D2D}}\right)\right]=\mathbb{E}\left[\prod_{\Phi_c}\exp\left(-sP_{c\,i}G_{c\,i}r_{c\,i}^{-\alpha_d}\right)\right], \tag{11}$$

with $P_{c\,i}$ representing the transmit power of the i^{th} interfering cellular UEs, $G_{c\,i}$ is the fading power gain on the i^{th} link and $r_{c\,i}$ is the distance of the i^{th} cellular UE from the RX under consideration. Due to the fact that the location of interfering cellular UEs is approximated by PPP with density λ_b and all fading are i.i.d., we can drop the index i. Then using the mapping theorem in which the Poisson process distributing the interferers in $\mathbb{R}^2$ can be mapped to $\mathbb{R}^+$ [18], we can rewrite $\mathcal{L}_{I_c^{\mathrm{D2D}}}(s)$ in (11) as

$$\begin{aligned}\mathcal{L}_{I_c^{\mathrm{D2D}}}(s)&=\exp\left(-\int_0^\infty \mathbb{E}_{P_c,G_c}\left[1-\exp\left(-sP_cG_cr^{-\alpha_d}\right)\right]2\pi\lambda_b r\mathrm{d}r\right)\\&=\exp\left(-2\pi\lambda_b\mathbb{E}_{P_c}\left[\int_0^\infty\left(1-\frac{1}{1+sP_cr^{-\alpha_d}}\right)r\,\mathrm{d}r\right]\right)\\&=\exp\left(-\pi\lambda_b\mathbb{E}\left[P_c^{\frac{2}{\alpha_d}}\right]s^{\frac{2}{\alpha_d}}\Gamma\left(1+\frac{2}{\alpha_d}\right)\Gamma\left(1-\frac{2}{\alpha_d}\right)\right),\end{aligned} \tag{12}$$

where the second step comes from the fact that G_c follows the exponential distribution, and $\Gamma(s)=\int_0^\infty t^{s-1}e^{-t}\mathrm{d}t$ is the gamma function. Note that the mode selection scheme has no impact on the interference from other cellular UEs, and so $\mathcal{L}_{I_c^{\mathrm{D2D}}}(s)$ will always be the same for all three mode selection schemes.

Next, we consider the case of D2D interference. For the *distance cut-off* scheme, whether potential D2D transmitters are in D2D mode depends on their distance to the D2D RXs only. In other words, the location of D2D UEs can be regarded as the independent thinning of the underlay PPP. As such, the density of these D2D UEs is $\mathbb{P}_{D2D}\lambda_d$. For the other two schemes, the selection of D2D mode also depends on the distance to the BSs, therefore, the location of D2D UEs is the dependent thinning of the underlay PPP. However, due to the complexity associated with modelling these D2D UEs, we assume that for the *link gain* scheme these D2D UEs still follow a PPP with density $\mathbb{P}_{D2D}\lambda_d$, while they follow a PPP with density λ_d under *guard zone* scheme because the interference is mainly governed by surrounding D2D UEs [14]. This allows us to maintain model tractability, which has also been assumed in the literature [13], [14]. The accuracy of this approximation will be illustrated in Section IV.

Following the same derivation process for $\mathcal{L}_{I_c^{\mathrm{D2D}}}(s)$, we have

$$\begin{aligned}\mathcal{L}_{I_d^{\mathrm{D2D}}}(s)&=\exp\left(-\int_0^\infty\frac{\mathbb{E}_{P_d,G_d}\left[1-\exp\left(-sP_dG_dr^{-\alpha_d}\right)\right]}{\mathbb{P}_{D2D}^{-1}}2\pi\lambda_d r\,\mathrm{d}r\right)\\&=\exp\left(-\pi\mathbb{P}_{D2D}\lambda_d\mathbb{E}\left[P_d^{\frac{2}{\alpha_d}}\right]s^{\frac{2}{\alpha_d}}\Gamma\left(1+\frac{2}{\alpha_d}\right)\Gamma\left(1-\frac{2}{\alpha_d}\right)\right).\end{aligned} \tag{13}$$

Note that, for the *guard zone* scheme, we need to replace $\mathbb{P}_{D2D}\lambda_d$ by λ_d, since the intensity of interfering D2D UEs is assumed to be λ_d for this case. Finally, substituting $\mathcal{L}_{I_c^{\mathrm{D2D}}}(s)$ and $\mathcal{L}_{I_d^{\mathrm{D2D}}}(s)$ with $s=\frac{\theta}{\rho}$ into (4), we obtain the result in *Theorem 1*.

Appendix B
Success Probability at the Base Station

In this appendix, we show how (4) can be evaluated for a typical BS. Similar to the interference experienced at the D2D RX, the interference experienced at the BS is the same for any mode selection scheme. Moreover, it is worth noting the closest a cellular interferer can be is distance R (i.e., the cellular residing in a neighbouring macrocell) due to orthogonalization of the channels. Taking into account this limit, $\mathcal{L}_{I_c^{\mathrm{BS}}}(s)$ for the typical BS is given by

$$\begin{aligned}\mathcal{L}_{I_c^{\mathrm{BS}}}(s)&=\exp\left(-\int_R^\infty\mathbb{E}_{P_c,G_c}\left[1-\exp\left(-sP_cG_cr^{-\alpha_c}\right)\right]2\pi\lambda_b r\,\mathrm{d}r\right)\\&=\exp\left(-2\pi\lambda_b\mathbb{E}_{P_c}\left[\frac{sP_{c}{}_2F_1\left(1,1-\frac{2}{\alpha_c};2-\frac{2}{\alpha_c};-sP_cR^{-\alpha_c}\right)}{(\alpha_c-2)R^{\alpha_c-2}}\right]\right)\\&=\exp\left(-2\pi\lambda_b\int_0^R{}_2F_1\left(1,1-\frac{2}{\alpha_c};2-\frac{2}{\alpha_c};-s\rho r_c^{\alpha_c}R^{-\alpha_c}\right)\frac{2r_c}{R^2}\,\mathrm{d}r_c\right)\\&=\exp\left(\frac{\pi\lambda_bR^2\theta}{(2-\alpha_c)(2+\alpha_c)}\left((2+\alpha_c){}_2F_1\left(1,1-\frac{2}{\alpha_c};2-\frac{2}{\alpha_c};-\theta\right)\right.\right.\end{aligned}$$

$$+(2-\alpha_c){}_2F_1\left(1,1+\frac{2}{\alpha_c};2+\frac{2}{\alpha_c};-\theta\right)\Big)\Big), \quad (14)$$

where the third step comes from the fact that $P_c=\rho r_c^{\alpha_c}$ and ${}_2F_1(\cdot,\cdot;\cdot;\cdot)$ is the hypergeometric function.

Now we calculate the value of $\mathcal{L}_{I_d^{\text{BS}}}\left(\frac{\theta}{\rho}\right)\equiv\exp\{A_{\mathcal{M}}\}$ for different $\mathcal{M}=1,2,3$. Since for certain mode selection schemes (i.e., $\mathcal{M}=2,3$), whether the potential D2D transmitters will generate interference to the BS or not also relies on their distance to the BS, we need to analyze the interference from D2D UEs separately.

Under the *distance cut-off* scheme, there is no limit on the distance between a D2D interferer and the typical BS. Following the same derivation procedure as (13), we obtain

$$\mathcal{L}_{I_d^{\text{BS}}}(s)=\exp\left(-\pi\mathbb{P}_{D2D}\lambda_d\mathbb{E}\left[P_d^{\frac{2}{\alpha_c}}\right]s^{\frac{2}{\alpha_c}}\Gamma\left(1+\frac{2}{\alpha_c}\right)\Gamma\left(1-\frac{2}{\alpha_c}\right)\right). \quad (15)$$

Under the *link gain* scheme, the D2D UE will generate interference to the typical BS if and only if $T_d r_d^{-\alpha_d}>r_c^{-\alpha_c}$. This implies that the distance of a D2D interferer from the BS has a lower bound given by $r_c>\left(\frac{r_d^{\alpha_d}}{T_d}\right)^{\frac{1}{\alpha_c}}=\left(\frac{P_d}{T_d\rho}\right)^{\frac{1}{\alpha_c}}$. Considering this bound, we have

$$\begin{aligned}\mathcal{L}_{I_d^{\text{BS}}}(s)&=\exp\left(\mathbb{E}_{P_d}\left[-\int_{\left(\frac{P_d}{T_d\rho}\right)^{\frac{1}{\alpha_c}}}^{\infty}\frac{\mathbb{E}_{G_d}\left[1-\exp\left(-sP_dG_dr^{-\alpha_c}\right)\right]}{\left(2\pi\mathbb{P}_{D2D}\lambda_d\right)^{-1}}r\mathrm{d}r\right]\right)\\
&=\exp\left(-\mathbb{E}_{P_d}\left[-\int_{\left(\frac{1}{sT_d\rho}\right)^{\frac{1}{\alpha_c}}}^{\infty}\left(\frac{y}{y^{\alpha_c}+1}\right)2\pi\mathbb{P}_{D2D}\lambda_d s^{\frac{2}{\alpha_c}}P_d^{\frac{2}{\alpha_c}}\mathrm{d}y\right]\right)\\
&=\exp\left(-2\pi\mathbb{P}_{D2D}\lambda_d\mathbb{E}\left[P_d^{\frac{2}{\alpha_c}}\right]s^{\frac{2}{\alpha_c}}\int_{\left(\frac{1}{sT_d\rho}\right)^{\frac{1}{\alpha_c}}}^{\infty}\left(\frac{y}{y^{\alpha_c}+1}\right)\mathrm{d}y\right)\\
&=\exp\left(-\frac{2\pi\mathbb{P}_{D2D}\lambda_d\mathbb{E}\left[P_d^{\frac{2}{\alpha_c}}\right]sT_d^{1-\frac{2}{\alpha_c}}\rho^{1-\frac{2}{\alpha_c}}}{(\alpha_c-2)\left({}_2F_1\left(1,1-\frac{2}{\alpha_c};2-\frac{2}{\alpha_c};-sT_d\rho\right)\right)^{-1}}\right),\end{aligned} \quad (16)$$

where the third step comes from using the property $\mathbb{E}_{G_d}[\exp(-sG_d)]=\frac{1}{1+s}$ and the substitution of $y=(sP_d)^{-\frac{1}{\alpha_c}}r$.

Under the *guard zone* scheme, the D2D interference can be modelled by splitting the region into two regions [14]. The first comprises the ring from the edge of the guard zone ($r_c=R_g$) to the edge of the guard zones of the adjacent macrocells ($r_c=2R-R_g$) with D2D density λ_d. The second part covers the rest of the area outside this ring and has intensity $\mathbb{P}_{D2D}\lambda_d$. Then, we have

$$\begin{aligned}\mathcal{L}_{I_d^{\text{BS}}}(s)&=\exp\Bigg(-\int_{R_g}^{2R-R_g}\mathbb{E}_{P_d,G_d}\left[1-\exp\left(-sP_dG_dr^{-\alpha_c}\right)\right]2\pi\lambda_d r\mathrm{d}r\\
&-\int_{2R-Rg}^{\infty}\mathbb{E}_{P_d,G_d}\left[1-\exp\left(-sP_dG_dr^{-\alpha_c}\right)\right]2\pi\mathbb{P}_{D2D}\lambda_d r\mathrm{d}r\Bigg)\\
&=\exp\Bigg(-2\pi\lambda_d\mathbb{E}_{P_d}\Big[\int_{R_g}^{\infty}\frac{sP_d}{r^{\alpha_c}+sP_d}r\,\mathrm{d}r\\
&-(1-\mathbb{P}_{D2D})\int_{2R-R_g}^{\infty}\frac{sP_d}{r^{\alpha_c}+SP_d}r\,\mathrm{d}r\Big]\Bigg)\\
&=\exp\Bigg(-2\pi\lambda_d\int_0^{R_{\max}}\Bigg(\frac{{}_2F_1\left(1,1-\frac{2}{\alpha_c};2-\frac{2}{\alpha_c};-s\rho r_d^{\alpha_d}R_g^{-\alpha_c}\right)}{(\alpha_c-2)\left(s\rho r_d^{\alpha_d}\right)^{-1}R_g^{\alpha_c-2}}\\
&-\frac{s\rho r_d^{\alpha_d}{}_2F_1\Big(1,1-\frac{2}{\alpha_c};2-\frac{2}{\alpha_c};-s\rho r_d^{\alpha_d}(2R-R_g)^{-\alpha_c}\Big)}{(\alpha_c-2)\left(1-\mathbb{P}_{D2D}\right)^{-1}(2R-R_g)^{\alpha_c-2}}\Bigg)f_{r_d}(r_d)\mathrm{d}r_d\Bigg),\end{aligned} \quad (17)$$

where the third step comes from $P_d=\rho r_d^{\alpha_d}$. Substituting the distribution of $f_{r_d}(r_d)$ given in (2) leads to the value of A_3 presented in (9). Combining (14)-(17), we obtain the results in *Theorem 2*.

REFERENCES

[1] P. Agyapong, M. Iwamura, D. Staehle, W. Kiess, and A. Benjebbour, "Design considerations for a 5G network architecture," *IEEE Commun. Mag.*, vol. 52, no. 11, pp. 65–75, Nov. 2014.

[2] A. Asadi, Q. Wang, and V. Mancuso, "A survey on device-to-device communication in cellular networks," *IEEE Commun. Surveys Tuts.*, vol. 16, no. 4, pp. 1801–1819, Fourth quarter 2014.

[3] C.-X. Wang, F. Haider, X. Gao, X.-H. You, Y. Yang, D. Yuan, H. Aggoune, H. Haas, S. Fletcher, and E. Hepsaydir, "Cellular architecture and key technologies for 5G wireless communication networks," *IEEE Commun. Mag.*, vol. 52, no. 2, pp. 122–130, Feb. 2014.

[4] X. Lin, J. Andrews, A. Ghosh, and R. Ratasuk, "An overview of 3GPP device-to-device proximity services," *IEEE Commun. Mag.*, vol. 52, no. 4, pp. 40–48, Apr. 2014.

[5] P. Janis, C. Yu, K. Doppler, C. Ribiero, C. Wijting, K. Higl, O. Tirkkonen, and V. Koivunen, "Device-to-device communication underlaying cellular communications systems," *Int'l J. of Communications, Network and System Sciences*, vol. 2, no. 3, pp. 169–178, 2009.

[6] M. Peng, Y. Li, T. Quek, and C. Wang, "Device-to-device underlaid cellular networks under rician fading channels," *IEEE Trans. Wireless Commun.*, vol. 13, no. 8, pp. 4247–4259, Aug. 2014.

[7] N. Lee, X. Lin, J. Andrews, and R. Heath, "Power control for D2D underlaid cellular networks: Modeling, algorithms, and analysis," *IEEE J. Sel. Areas Commun.*, vol. 33, no. 1, pp. 1–13, Jan. 2015.

[8] M. Jung, K. Hwang, and S. Choi, "Joint mode selection and power allocation scheme for power-efficient device-to-device (D2D) communication," in *Proc. IEEE VTC Spring*, May. 2012, pp. 1–5.

[9] P. Cheng, L. Deng, H. Yu, Y. Xu, and H. Wang, "Resource allocation for cognitive networks with d2d communication: An evolutionary approach," in *Proc. IEEE WCNC*, Apr. 2012, pp. 2671–2676.

[10] G. Yu, L. Xu, D. Feng, R. Yin, G. Li, and Y. Jiang, "Joint mode selection and resource allocation for device-to-device communications," *IEEE Trans. Commun.*, vol. 62, no. 11, pp. 3814–3824, Nov. 2014.

[11] L. Lei, X. Shen, M. Dohler, C. Lin, and Z. Zhong, "Queuing models with applications to mode selection in device-to-device communications underlaying cellular networks," *IEEE Trans. Wireless Commun.*, vol. 13, no. 12, pp. 6697–6715, Dec. 2014.

[12] X. Lin, J. G. Andrews, and A. Ghosh, "Spectrum sharing for device-to-device communication in cellular networks," *IEEE Trans. Wireless Commun.*, vol. 13, no. 12, pp. 6727–6740, Dec. 2014.

[13] H. ElSawy, E. Hossain, and M.-S. Alouini, "Analytical modeling of mode selection and power control for underlay D2D communication in cellular networks," *IEEE Trans. Commun.*, vol. 62, no. 11, pp. 4147–4161, Nov. 2014.

[14] J. Ye and Y. J. Zhang, "A guard zone based scalable mode selection scheme in D2D underlaid cellular networks," *arXiv technical report*, 2014. [Online]. Available: http://arxiv.org/abs/1406.7395

[15] T. Rappaport, *Wireless Communications: Principles and Practice*, ser. Prentice Hall, 2009.

[16] F. Baccelli and B. Blaszczyszyn, *Stochastic Geometry and Wireless Networks: Volume 1: THEORY*, ser. Foundations and Trends(r) in Networking. Now Publishers, 2009.

[17] J. Guo, S. Durrani, and X. Zhou, "Performance analysis of arbitrarily-shaped underlay cognitive networks: Effects of secondary user activity protocols," *IEEE Trans. Commun.*, vol. 63, no. 2, pp. 376–389, Feb. 2015.

[18] M. Haenggi, *Stochastic Geometry for Wireless Networks*. Cambridge University Press, Oct. 2012.